



The Influence of Secondary Electron Emission in the Dust Charging Process

Sanchari Mukherjee¹, Rajarshi Nath², Snehangshu Mahapatra² and Samit Paul³

Faculty, Department of Basic Science and Humanities, Narula Institute of Technology, Kolkata, India¹

Student, Department of Computer Science and Engineering, Narula Institute of Technology, Kolkata, India²

Faculty, Natagarh Sri Sri Ramkrishna Vidyamandir, Kolkata, India³

Abstract: In this paper, the dust charging process is investigated in the presence of suprathermal primary and secondary electrons. A simplified model for dusty plasmas is adopted, whose constituents are suprathermal inertialess primary electrons, secondary electrons, inertial ions, and charged immobile dust grains. The suprathermal primary electrons and secondary electrons are assumed to follow the Lorentzian kappa velocity distribution. Expressions of secondary electron currents are derived considering negatively and positively charged dust grains. Numerical analysis shows that the suprathermal electron population has a significant effect on secondary electron emission currents.

Keywords: Dusty plasma, Secondary emission, Lorentzian plasma

I. INTRODUCTION

Space and astrophysical plasmas are made of ions and electrons along with small dust grains. These small dust grains are very large comparing ions and electrons and they may accumulate charge by attachment or emission of electrons and ions. It is also observed that when small dust grains come to exposure of ultraviolet rays, they emit electrons from the dust grain surface [1-4]. Similarly, the electrons emit due to the excited hitting of electrons on the dust grains surface. This is the secondary electron emission. The secondary emission of electrons is one of the emission processes that may play an important role in dust grain charging because electron emission acts as a positive current to the dust particle [5-14]. The electron and ion plasma charging current densities and secondary electron current density have been previously presented [1,8,15] with the Maxwellian distribution. Jingyu Gong and Jiulin Du discussed the dust charging process with nonextensive power law distribution and the effect of secondary electron emission on this charging process [16,17].

In this paper, we investigate the dust charging process in the presence of both the suprathermal primary and secondary electrons. We study in detail the influences of the suprathermal population on secondary electron emission current and analyze the balance situation of total current. The suprathermal electron population has a significant influence on total current. Both the negative and positive nature of the dust grain charge is considered. The effect of both the population of secondary electrons and the population of suprathermal electrons in Lorentzian dusty plasma are studied numerically.

II. PLASMA CURRENTS

In dusty plasma, dust charge varies due to the attachment of electrons and ions to the dust grain. Secondary electron emission may also work as a positive charge flux to the dust grains. The flux of electrons and ions is also influenced by the dust grain surface potential. Since the variation of the flux of electrons and ions influences the dust charge, it is also called charging current. Using the orbit-limited motion approach, the charging current for electrons and ions can be calculated if the radius of the dust grain is smaller than the Debye radius [18].

Now we consider that electrons and ions obey the Lorentzian kappa velocity distribution function [19]

$$f_{\alpha 0}(E) = n_{\alpha 0} \left(\frac{m_{\alpha}}{2\pi\kappa_{\alpha} E_0} \right)^{3/2} \frac{\Gamma(\kappa_{\alpha} + 1)}{\Gamma(\kappa_{\alpha} - 1/2)} \left[1 + \frac{E}{\kappa_{\alpha} E_0} \right]^{-(\kappa_{\alpha} + 1)}, \quad \alpha = e, i \quad (1)$$

where $E_0 = \left[\frac{(2\kappa_{\alpha} - 3)T_{\alpha}}{\kappa_{\alpha}} \right]$. m_{α} , $n_{\alpha 0}$, T_{α} are respectively the mass, number density, temperature, and E is the energy of the



corresponding particles, Γ is the Gamma function. κ_α is the kappa index. $\alpha = e, i$, e and i indicates the electrons and ions respectively. Using this velocity distribution function, the electron, ion, and secondary electron charging currents are already been derived in Lorentzian dusty plasma [15]:

$$I_e = -\pi r_0^2 n_e \left(\frac{8T_e}{\pi m_e} \right)^{\frac{1}{2}} \left(\kappa_e - \frac{3}{2} \right)^{\frac{1}{2}} \frac{\Gamma(\kappa_e - 1)}{\Gamma\left(\kappa_e - \frac{1}{2}\right)} \left(1 - \frac{eq_d}{r_0 \left(\kappa_e - \frac{3}{2}\right) T_e} \right)^{-(\kappa_e - 1)} \quad \phi \leq 0 \quad (2)$$

$$I_e = -\pi r_0^2 n_e \left(\frac{8T_e}{\pi m_e} \right)^{\frac{1}{2}} \left(\kappa_e - \frac{3}{2} \right)^{\frac{1}{2}} \frac{\Gamma(\kappa_e - 1)}{\Gamma\left(\kappa_e - \frac{1}{2}\right)} \left(1 + \frac{eq_d (\kappa_e - 1)}{r_0 \left(\kappa_e - \frac{3}{2}\right) T_e} \right) \quad \phi \geq 0 \quad (3)$$

$$I_i = \pi r_0^2 n_i \left(\frac{8T_i}{\pi m_i} \right)^{\frac{1}{2}} \left(\kappa_i - \frac{3}{2} \right)^{\frac{1}{2}} \frac{\Gamma(\kappa_i - 1)}{\Gamma\left(\kappa_i - \frac{1}{2}\right)} \left(1 - \frac{eq_d (\kappa_i - 1)}{r_0 \left(\kappa_i - \frac{3}{2}\right) T_i} \right) \quad \phi \leq 0 \quad (4)$$

$$I_i = \pi r_0^2 n_i \left(\frac{8T_i}{\pi m_i} \right)^{\frac{1}{2}} \left(\kappa_i - \frac{3}{2} \right)^{\frac{1}{2}} \frac{\Gamma(\kappa_i - 1)}{\Gamma\left(\kappa_i - \frac{1}{2}\right)} \left(1 + \frac{eq_d}{r_0 \left(\kappa_i - \frac{3}{2}\right) T_i} \right)^{-(\kappa_i - 1)} \quad \phi \geq 0 \quad (5)$$

$$I_s = 4\pi r_0^2 n_e \left(\frac{1}{2\pi\kappa_e^3 E_0^3} \right)^{1/2} \frac{\Gamma(\kappa_e + 1)}{\Gamma(\kappa_e - 1/2)} \int_0^\infty E \delta(E) \left[1 + \frac{E - e\phi}{\kappa_e E_0} \right]^{-\kappa_e - 1} dE, \quad \phi \leq 0 \quad (6)$$

$$I_s = 4\pi r_0^2 n_e \left(\frac{1}{2\pi\kappa_e^3 E_0^3} \right)^{1/2} \frac{\Gamma(\kappa_e + 1)}{\Gamma(\kappa_e - 1/2)} \left(1 + \frac{e\phi}{T_s} \right) \times \exp\left(\frac{-e\phi}{T_s}\right) \int_{e\phi}^\infty E \delta(E) \left[1 + \frac{E - e\phi}{\kappa_e E_0} \right]^{-\kappa_e - 1} dE, \quad \phi \geq 0 \quad (7)$$

Here E is the impact energy and ϕ is the dust surface potential. The dust grain surface potential $\phi = q_d / r_0$, where q_d and r_0 are charge and radius of the dust grains. T_s is the temperature of the secondary electrons. Here we assume the uniform spherical shape of the dust grains. To derive the current due to secondary electron emission from the equation (5) and (6), we consider that the expression of the secondary yield due to electron impact is [1]

$$\delta(E) = 7.4 \delta_M \frac{E}{E_M} \exp\left(-2\sqrt{E/E_M}\right) \quad (8)$$

where δ_M is the maximum value of δ . The quantities δ_M and E_M are determined by the materials of dust grains. It is clear from the above equations that the expression of current depends on the nature of the surface potential of dust grains (ϕ). Using the yield function from equation (8), we obtain the current expressions due to secondary electron emission, when $\phi < 0$, as follows:

$$I_e^s = 3.7\pi r_0^2 \delta_M n_e \left(\frac{8T_s}{\pi m_e} \right)^{\frac{1}{2}} \frac{\Gamma(\kappa_e + 1)}{\left(\kappa_e - \frac{3}{2}\right)^{\frac{3}{2}} \Gamma\left(\kappa_e - \frac{1}{2}\right)} F_{\kappa_e}^-(U, x) \quad (9)$$

where

$$F_{\kappa_e}^-(U, x) = x^2 \int_0^\infty u^5 e^{-u} \left\{ 1 + \frac{xu^2 - U}{\left(\kappa_e - \frac{3}{2}\right)} \right\}^{-(\kappa_e + 1)} du \quad (10)$$



Here $U = \frac{eq_d}{r_0 T_e}$ and $x = \frac{E_M}{4T_e}$.

Now when the dust surface potential is positive ($\phi > 0$), the expression of current is obtained from equation (7) using equation (8):

$$I_e^s = 3.7\pi r_0^2 \delta_M n_e \left(\frac{8T_s}{\pi m_e} \right)^{\frac{1}{2}} \frac{\Gamma(\kappa_e + 1)}{\left(\kappa_e - \frac{3}{2} \right)^{\frac{3}{2}} \Gamma\left(\kappa_e - \frac{1}{2}\right)} \left(1 + \frac{U}{\sigma_s} \right) \exp\left(-\frac{U}{\sigma_s} \right) F_{\kappa^+}(U, x) \quad (11)$$

Where

$$F_{\kappa^+}(U, x) = x^2 \int_B^{\infty} u^5 e^{-u} \left\{ 1 + \frac{xu^2 - U}{\left(\kappa_e - \frac{3}{2} \right)} \right\}^{-(\kappa_e + 1)} du \quad (12)$$

where $\sigma_s = T_s / T_e$ and the lower limit of the integration $B = \sqrt{U / x}$.

The functions $F_{\kappa^-}(U, x)$ and $F_{\kappa^+}(U, x)$ can be determined numerically for different parameter values.

III. NET CURRENT AND EQUILIBRIUM DUST CHARGE

The dust charge q_d is variable due to the variation of the current flow to the dust surface. Thus, the variable dust charge q_d satisfies the grain charging equation

$$\frac{\partial q_d}{\partial t} = I_e + I_i + I_e^s \quad (13)$$

The net current to the dust grain is zero in the equilibrium condition. We obtain two expressions of net current considering two natures of dust grain potential. The normalized form of the net currents in the case of native and positive dust grains respectively are

$$\begin{aligned} I_{net}^- &= I_e + I_i + I_e^s \\ &= -\left(\kappa_e - \frac{3}{2} \right)^{\frac{1}{2}} \frac{\Gamma(\kappa_e - 1)}{\Gamma\left(\kappa_e - \frac{1}{2}\right)} \left(1 - \frac{U}{\left(\kappa_e - \frac{3}{2} \right)} \right)^{-(\kappa_e - 1)} \\ &\quad + \left(k_i - \frac{3}{2} \right)^{\frac{1}{2}} \frac{\Gamma(k_i - 1)}{\Gamma\left(k_i - \frac{1}{2}\right)} \sqrt{\mu_i} \left(1 - \frac{U(k_i - 1)}{\sigma_i \left(k_i - \frac{3}{2} \right)} \right) \\ &\quad + 3.7\delta_M \frac{\Gamma(\kappa_e + 1)}{\left(\kappa_e - \frac{3}{2} \right)^{\frac{3}{2}} \Gamma\left(\kappa_e - \frac{1}{2}\right)} F_{\kappa^-}(U, x) \end{aligned} \quad (14)$$



$$\begin{aligned}
 I_{net}^+ &= I_e + I_i + I_e^s \\
 &= -\left(k_e - \frac{3}{2}\right)^{\frac{1}{2}} \frac{\Gamma(k_e - 1)}{\Gamma\left(k_e - \frac{1}{2}\right)} \left(1 + \frac{U(k_e - 1)}{\left(k_e - \frac{3}{2}\right)}\right) \\
 &\quad + \left(k_i - \frac{3}{2}\right)^{\frac{1}{2}} \frac{\Gamma(k_i - 1)}{\Gamma\left(k_i - \frac{1}{2}\right)} \sqrt{\frac{\sigma_i}{\mu_i}} \left(1 + \frac{U}{\sigma_i\left(k_i - \frac{3}{2}\right)}\right)^{-(k_i-1)} \\
 &\quad + 3.7\delta_M \frac{\Gamma(\kappa_e + 1)}{\left(\kappa_e - \frac{3}{2}\right)^{\frac{3}{2}} \Gamma\left(\kappa_e - \frac{1}{2}\right)} \left(1 + \frac{U}{\sigma_s}\right) \exp\left(-\frac{U}{\sigma_s}\right) F_{\kappa}^+(U, x)
 \end{aligned} \tag{15}$$

If $U < 0$, we have to use equation **Error! Reference source not found.** and for $U > 0$ we use (15).

IV. NUMERICAL RESULTS AND DISCUSSIONS

To obtain a better insight into the role of the secondary electrons on the dust charging procedure and the dust ion-acoustic wave propagation in the Lorentzian plasmas, we have performed an analytical derivation of the charging currents and the dust ion-acoustic wave frequency considering both the negative and positive dust grain in equilibrium. To assess the analytical results in a physical situation, we have considered the space plasmas containing suprathermal electrons e.g. solar wind, interplanetary space, cometary tails, etc. [20-22]. We have considered the value of the Kappa index between 2 and 6, as this range has been found to fit the observations in the astrophysical plasma [22]. For numerical estimation, we have considered the plasma parameters [17,23,24] $\sigma_i = 0.01-1$, $\sigma_s = 1-1.5$, $\delta_s = 0.1-1$, $r_0 / \lambda_{De} \approx 5 \times 10^{-4}$. Our main focus is on the effect of secondary electron emission and suprathermal electrons on the dust charging process and the influence of this charge variation on dust ion-acoustic wave propagation characteristics.

To calculate the secondary emission current (I_e^s), we calculated the core integral in the secondary emission current $F_{\kappa}^-(U, x)$ and $F_{\kappa}^+(U, x)$ numerically. Here we assume $U = -1$ for plotting $F_{\kappa}^-(U, x)$ and $U = 1$ for plotting $F_{\kappa}^+(U, x)$ as a function of x . Figures 1 and 2 show the variation of these two functions with x . Both function initially grows rapidly and then decreases slowly with increasing x . Comparing both figures we see that $F_{\kappa}^+(U, x)$ is greater than $F_{\kappa}^-(U, x)$. In Figures 2 and 3 we have plotted only the secondary current (I_{total}) as a function of U . The curves are plotted using equation **Error! Reference source not found.** when $U < 0$ and equation **Error! Reference source not found.** when $U > 0$. It shows that the current decreases with increasing kappa indices. So secondary current increases with increasing suprathermal electrons.

We plot the total current ($I_{total} = I_e + I_i + I_e^s$) as a function of dust surface potential (U). The numerical calculation of the total current is done using the equation **Error! Reference source not found.** for $U < 0$ and equation **Error! Reference source not found.** for $U > 0$. In equilibrium condition, we plot this total current (I_{total}) in Figure 5 for different values of the Kappa index (κ_e). We consider the other parameters $\sigma_i = 1$, $\sigma_s = 1.5$, $\delta_M = 5$ and $E_M / 4T = 45.6$. The figure shows that I_{total} decreases with increasing potential (U) and I_{total} becomes zero at some negative value of U . So equilibrium current balance condition indicates that the dust surface potential will be negative. On the other hand, figure 6 is plotted considering $\delta_M = 15$ keeping all the other parameters the same as figure 5. It shows that the current gradually decreases with increasing U . It also shows that current decreases with increasing kappa indices and approaches to the Maxwellian one. It shows that only the Maxwellian plot cuts the x-axis thrice, whereas suprathermal plots have only one cut on positive U . So we can have the only stable solution for suprathermal currents. So we may conclude that lower δ_M have a high probability of obtaining negative dust whereas high δ_M may give positive dust.

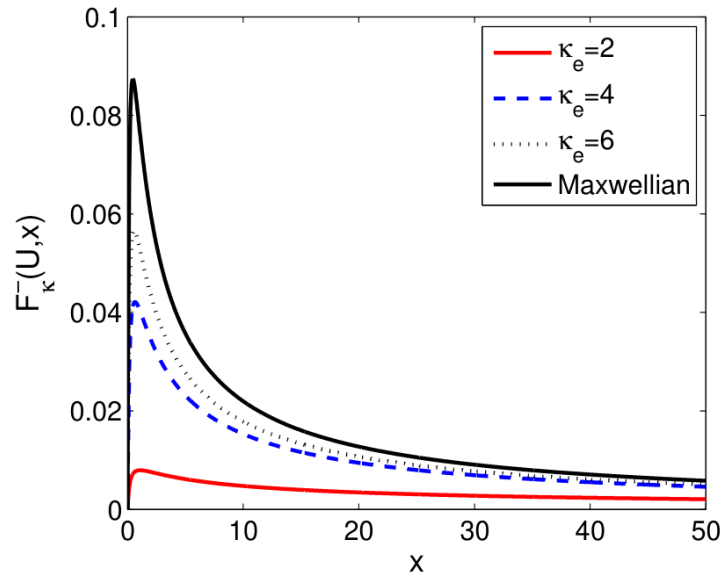


Fig. 1 Plot of $F_{\kappa}^{-}(U, x)$ versus x , considering $U = -1$. Other parameters are $\sigma_i = 1, \sigma_s = 1.5, \delta_M = 15$ and $E_M / 4T = 45.6$.

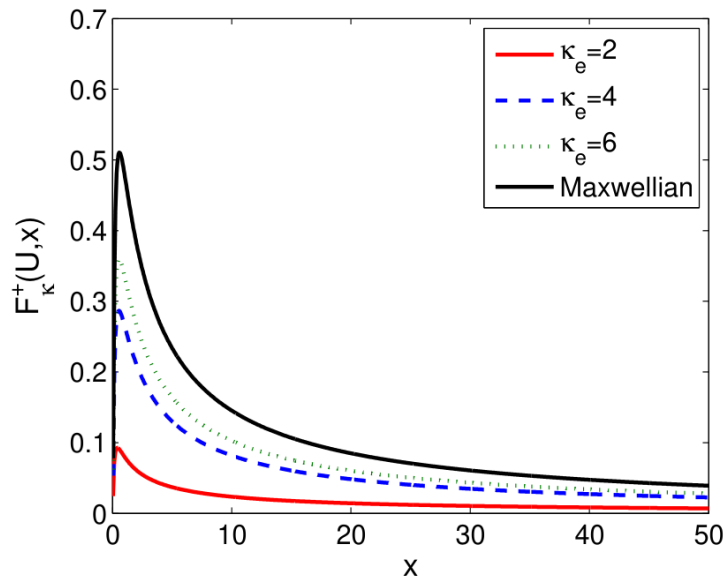


Fig. 2 Plot of $F_{\kappa}^{+}(U, x)$ versus x , considering $U = +1$ for different kappa index (κ_e). Other parameters are $\sigma_i = 1, \sigma_s = 1.5, \delta_M = 15$ and $E_M / 4T = 45.6$.

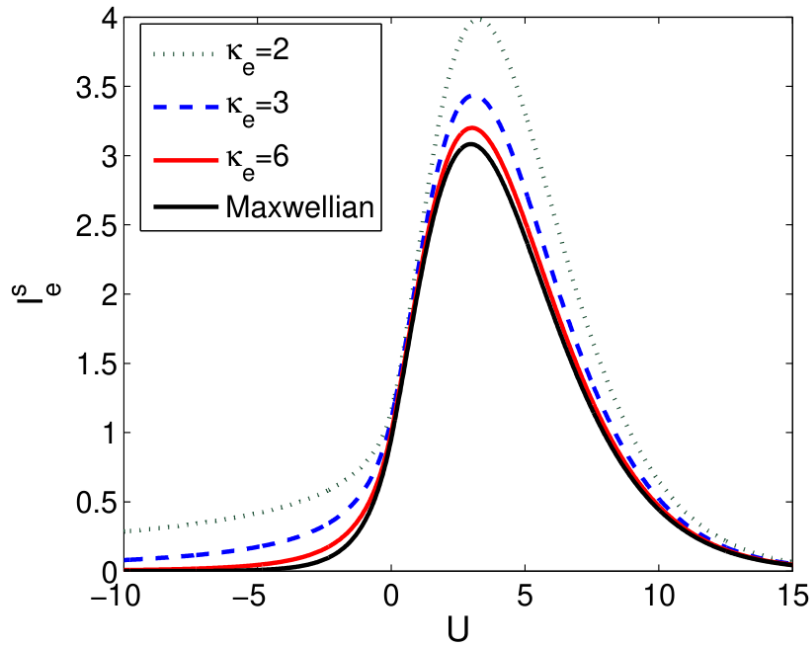


Fig. 3 Plot of secondary current (I_e^s) versus U for different electron kappa index (κ_e). Other parameters are $\sigma_i = 1$, $\sigma_s = 1.5$, $\delta_M = 15$ and $E_M / 4T = 45.6$.

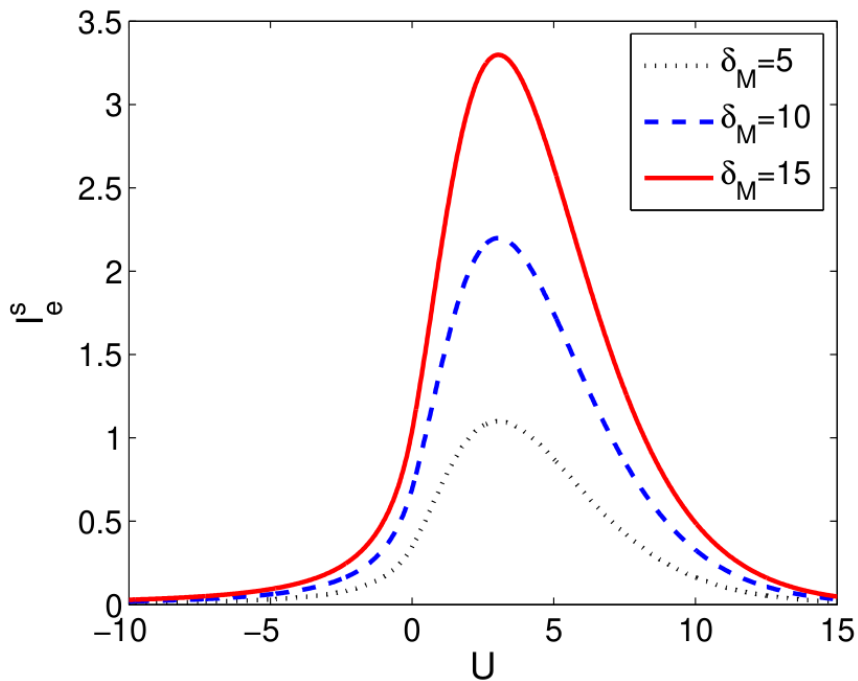


Fig. 4 Plot of secondary current (I_e^s) versus U for different δ_M , where $\sigma_i = 1$, $\sigma_s = 1.5$, $\kappa_e = 4$ and $E_M / 4T = 45.6$.

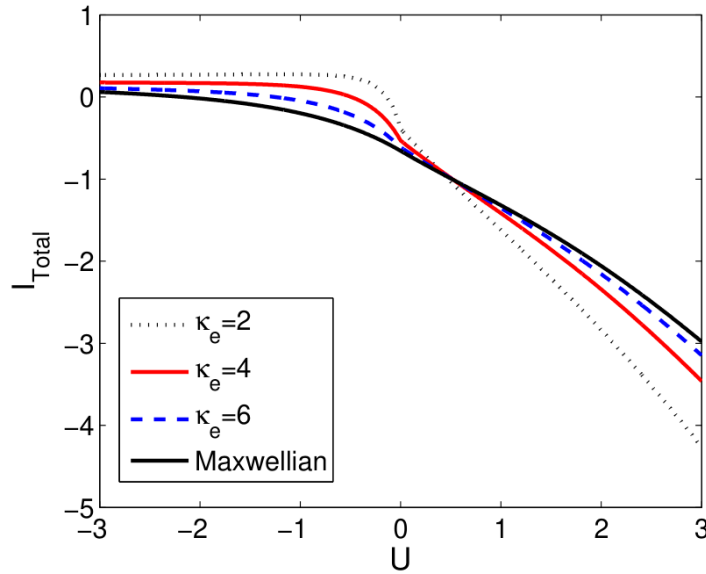


Fig. 5 Plot of total normalized current ($I_{total} = I_e + I_i + I_e^s$) versus normalized dust surface potential U for different kappa index (κ_e) considering $\sigma_i = 1, \sigma_s = 1.5, \delta_M = 5$ and $E_M / 4T = 45.6$.

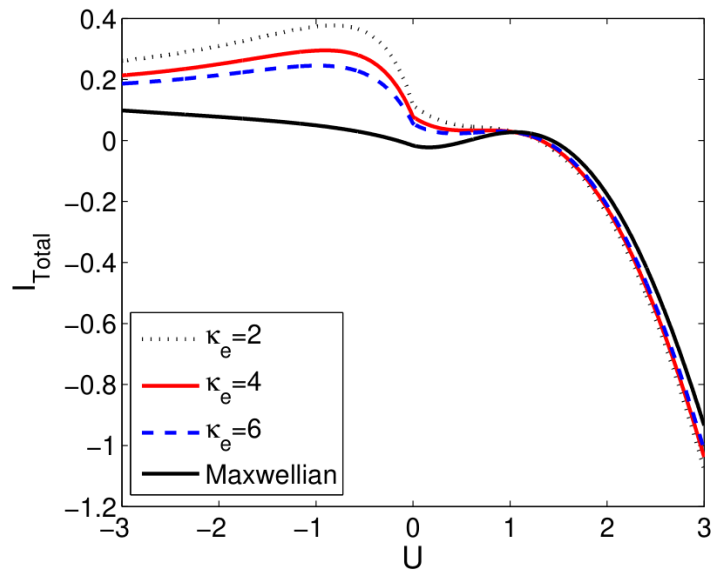


Fig. 6 Plot of total normalized current ($I_{total} = I_e + I_i + I_e^s$) versus normalized dust surface potential U for different kappa index (κ_e) considering $\sigma_i = 1, \sigma_s = 1.5, \delta_M = 15$ and $E_M / 4T = 45.6$.

V. CONCLUSION

An analytical theory on the effect of secondary electron emission on the dust charging process in the Lorentzian dusty plasmas is presented in this article. Suprathermal electrons are outlined by Lorentzian Kappa distribution. Secondary electron currents have been derived considering Lorentzian electrons and ions. A detailed discussion on the effect of suprathermal electrons on secondary electron emission current is presented. It shows that suprathermal electrons induce secondary electron emission. The secondary electron current increases with an increasing suprathermal electron population. The electron and ion attachment and impact make the dust charge variable. In the balanced condition, the potential of dust grains may be either negative or positive. These dust charging currents are calculated using negative and positive charge flux to the dust grains.



REFERENCES

- [1] Meyer-Vernet N. (1982). Flip-flop of electric potential of dust grains in space. *Astronomy and Astrophysics*, 105, 98–106.
- [2] Horányi M., Robertson S. and Walch B. (1995). Electrostatic charging properties of simulated lunar dust. *Geophysical Research Letters*, 22(16), 2079–2082.
- [3] Walch B., Horányi M. and Robertson S. (1995). Charging of Dust Grains in Plasma with Energetic Electrons. *Physical Review Letters*, 75(5), 838–841.
- [4] Bringol L. A. and Hyde T. W. (1997). Charging in a dusty plasma. *Advances in Space Research*, 20(8), 1539–1542.
- [5] Draine B. T. and Salpeter E. E. (1979). On the physics of dust grains in hot gas. *The Astrophysical Journal*, 231, 77–94.
- [6] Sternglass E. J. (1957). Theory of Secondary Electron Emission Under Electron Bombardment. Scientific Paper 6-94410-2-P9 (No. NP-8163). Westinghouse Electric Corp. Research Labs., Pittsburgh.
- [7] Zilavy P., Sternovský Z., Čermák I., Němeček Z. and Šafránková J. (1998). Surface potential of small particles charged by the medium-energy electron beam. *Vacuum*, 50(1), 139–142.
- [8] Goertz C. K. (1989). Dusty plasmas in the solar system. *Reviews of Geophysics*, 27(2), 271–292.
- [9] Horányi M. (1996). Charged Dust Dynamics in the Solar System. *Annual Review of Astronomy and Astrophysics*, 34(1), 383–418.
- [10] Khrapak S. A. and Morfill G. (2001). Waves in two component electron-dust plasma. *Physics of Plasmas*, 8(6), 2629–2634.
- [11] Shukla P. K. (2000). Dust acoustic wave in a thermal dusty plasma. *Physical Review E*, 61(6), 7249–7251.
- [12] Chakraborty M., Kausik S. S., Saikia B. K., Kakati M. and Bujarbarua S. (2003). The effect of the ambient plasma conditions on the variation of charge on dust grains. *Physics of Plasmas*, 10(2), 554–557.
- [13] Bruining H. (1954). *Physics and applications of secondary electron emission*. London: Pergamon Press.
- [14] Richterova I., Nemecek Z., Safrankova J. and Pavlu J. (2004). A Model of Secondary Emission From Dust Grains and Its Comparison With an Experiment. *IEEE Transactions on Plasma Science*, 32(2), 617–622.
- [15] Chow V. W., Mendis D. A. and Rosenberg M. (1993). Role of grain size and particle velocity distribution in secondary electron emission in space plasmas. *Journal of Geophysical Research: Space Physics*, 98(A11), 19065–19076.
- [16] Gong J. and Du J. (2012). Dust charging processes in the nonequilibrium dusty plasma with nonextensive power-law distribution. *Physics of Plasmas*, 19(2), 023704.
- [17] Gong J. and Du J. (2012). Secondary electron emissions and dust charging currents in the nonequilibrium dusty plasma with power-law distributions. *Physics of Plasmas*, 19, 063703.
- [18] Allen J. E. (1992). Probe theory - the orbital motion approach. *Physica Scripta*, 45(5), 497–503.
- [19] Summers D. and Thorne R. M. (1991). The modified plasma dispersion function. *Physics of Fluids B: Plasma Physics*, 3(8), 1835–1847.
- [20] Zouganelis I. (2008). Measuring suprathermal electron parameters in space plasmas: Implementation of the quasi-thermal noise spectroscopy with kappa distributions using in situ Ulysses/URAP radio measurements in the solar wind. *Journal of Geophysical Research: Space Physics*, 113(A8).
- [21] Vasyliunas V. M. (1968). A survey of low-energy electrons in the evening sector of the magnetosphere with OGO 1 and OGO 3. *Journal of Geophysical Research* (1896-1977), 73(9), 2839–2884.
- [22] Pierrard V. and Lazar M. (2010). Kappa Distributions: Theory and Applications in Space Plasmas. *Solar Physics*, 267(1), 153–174.
- [23] Paul S., Denra R. and Sarkar S. (2019). Study of Dust Acoustic Wave Propagation in a Lorentzian Dusty Plasma in Presence of Secondary Electron Emission. *Brazilian Journal of Physics*, 49(5), 738–744.
- [24] Baluku T. K. and Hellberg M. A. (2015). Kinetic theory of dust ion acoustic waves in a kappa-distributed plasma. *Physics of Plasmas*, 22(8), 083701.